

# Dalton Transactions

Accepted Manuscript



This is an *Accepted Manuscript*, which has been through the Royal Society of Chemistry peer review process and has been accepted for publication.

*Accepted Manuscripts* are published online shortly after acceptance, before technical editing, formatting and proof reading. Using this free service, authors can make their results available to the community, in citable form, before we publish the edited article. We will replace this *Accepted Manuscript* with the edited and formatted *Advance Article* as soon as it is available.

You can find more information about *Accepted Manuscripts* in the [Information for Authors](#).

Please note that technical editing may introduce minor changes to the text and/or graphics, which may alter content. The journal's standard [Terms & Conditions](#) and the [Ethical guidelines](#) still apply. In no event shall the Royal Society of Chemistry be held responsible for any errors or omissions in this *Accepted Manuscript* or any consequences arising from the use of any information it contains.

## COMMUNICATION

# Tuning luminescence behaviors of a chloroplatinum(II) complex by component exchanges of dynamic acylhydrazone bond

Cite this: DOI: 10.1039/x0xx00000x

Received 00th January 2012,  
Accepted 00th January 2012

DOI: 10.1039/x0xx00000x

www.rsc.org/

Jianjun Liang, Huanting Huang, Lipeng He, Nijuan Liu, Yanhuan Chen and Weifeng Bu\*

**A cationic chloroplatinum(II) complex was found to show remarkable luminescence enhancement upon self-assembly with tripodal dynamic acylhydrazone-bridged sulfonates in water. The successive exchange reactions with acylhydrazine or aldehyde resulted in a controllable decrease in the luminescence intensities.**

Dynamic acylhydrazone bonds can respond to external stimuli and undergo three types of thermodynamically controlled reactions: hydrolysis, component exchange and metathesis.<sup>1</sup> The formation and transformation of acylhydrazone bonds thus allow the reaction systems to selectively amplify the desired compounds at the expense of the unstable ones from the equilibrium distribution under acid-catalyzed conditions.<sup>2</sup> Because of this controllable performance, they have been designed to act as self-sorting and self-healing knots in the synthesis of medicines,<sup>3</sup> molecule-devices,<sup>4</sup> and smart materials.<sup>5</sup>

On the other hand, square-planar  $d^8$  platinum(II) complexes with  $N^4N^4N$  ligands tend to arrange themselves into oligomeric structures in both solid and solution states via metal-metal and/or ligand aromatic  $\pi$ - $\pi$  stacking interactions.<sup>6,7</sup> They show controllable spectroscopic and luminescence properties through controllably tuning the above-mentioned intermolecular interactions. Therefore, their aggregation-induced luminescence behavior has resulted in many potential applications in the fields of chemical sensors and electro-optical devices in the past decade.<sup>7</sup> However, stepwise tunable optical outputs of chloroplatinum(II) complexes ( $[Pt(N^4N^4N)Cl]^+Cl^-$ ) have only rarely been explored.<sup>8</sup>

When cationic chloroplatinum(II) complexes self-assembled with anionic species such as block copolymers,<sup>8b</sup> surfactants<sup>8c</sup> and  $PF_6^-$ ,<sup>9</sup> they were found to show remarkable luminescence enhancement. In an effort to achieve tunable photophysical properties, dynamic acylhydrazone bonds and chloroplatinum(II)

complexes were meshed into a single system (Fig. 1). We therefore synthesized a series of water-soluble compounds, including a chloroplatinum(II) complex of 2,6-bis(benzimidazol-2'-yl)pyridine bearing two hexaethylene glycol methyl ether groups (**Pt-bzimpy**), tripodal hydrazone-linked sodium benzene sulfonate (**T**), benzoyl hydrazine (**H1**), tripodal acylhydrazine (**H2**), benzaldehyde with a hexaethylene glycol methyl ether group (**A1**), sodium 2-formylbenzenesulfonate (**A2**), and single hydrazone-bridged sodium benzene sulfonate (**S**). To the best of our knowledge, these compounds comprise the first luminescence-tunable library created via component exchange reactions of the acylhydrazones with the hydrazines or aldehydes.

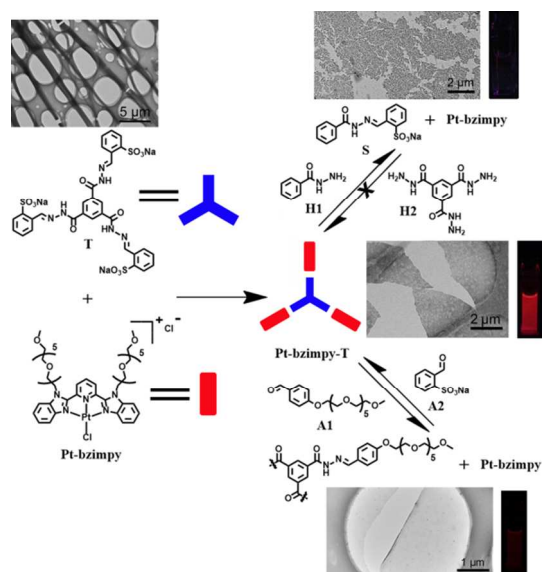


**Fig. 1** Controllable luminescence behaviors of a chloroplatinum(II) complex (**Pt-bzimpy**) driven by component exchanges of dynamic acylhydrazone bonds.

The aggregation of the  $C_3$ -symmetrical discotic **T** in water was clearly evidenced by both dynamic light scattering (DLS) and transmission electron microscopy (TEM). In a typical DLS plot for the aqueous solution of **T** (0.15 mM), three modes were detected at hydrodynamic diameters ( $D_h$ s) of 390, 4300, and 9100 nm (Fig. 2a), much larger than the molecular size of **T** (ca. 2 nm). Correspondingly, long fibres with a width of ~300 nm and lengths of 10~100  $\mu$ m were observed by TEM imaging (Fig. 2b). Similar nanofibres were also formed by discotic compounds with a benzene-1,3,5-tricarboxamide core via tripodal N-H...O hydrogen bonds and  $\pi$ - $\pi$  interactions.<sup>10</sup>

The UV-vis spectrum of **Pt-bzimpy** in an aqueous solution (0.45 mM) showed a broad absorption band at 400~490 nm and a low-energy absorption shoulder at 553 nm with moderate intensities (Fig. 3a). In accordance with previous spectroscopic studies on chloroplatinum(II) complexes,<sup>6-8</sup> the former band was assigned to a metal-to-ligand charge transfer transition (MLCT [ $d\pi(\text{Pt}) \rightarrow \pi^*(\text{bzimpy})$ ]). The later was regarded as a typical metal-metal-to-ligand charge transfer transition (MMLCT [ $d\sigma^*(\text{Pt}) \rightarrow \pi^*(\text{bzimpy})$ ]), originating from an intermolecular association through Pt...Pt and  $\pi$ - $\pi$  stacking interactions. Upon excitation at 420 nm, the emission spectrum showed a weak structureless band centered at 632 nm in air atmosphere (Fig. 3b). This emission band was accordingly attributed to a <sup>3</sup>MMLCT excited state.

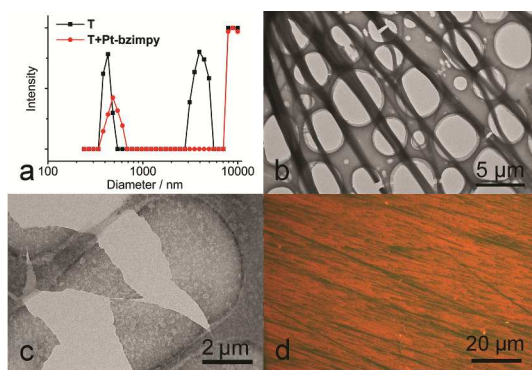


**Fig. 2** (a) DLS plots of **T** in its aqueous solution (0.15 mM) before (black) and after addition of **Pt-bzimpy** (3 equiv, red). TEM images of **T** before (b) and after addition of **Pt-bzimpy** (c). (d) Fluorescence microscope image of **T** upon addition of **Pt-bzimpy**.

When the solution of **Pt-bzimpy** was titrated with **T**, the MLCT absorption gradually decreased in its intensity. By contrast, the MMLCT band at 553 nm rose with **T** (Fig. 3a). A well-defined isosbestic point was observed at 495 nm. The maximum absorption intensity of the MMLCT band was achieved at a molar ratio of 0.31 between **T** and **Pt-bzimpy**, close to their charge ratio (1:3, Fig. 3c). In the corresponding emission spectra, the luminescence intensity of the <sup>3</sup>MMLCT band at 632 nm increased stepwise to a maximum value at a **T/Pt-bzimpy** molar ratio of 0.35 (Fig. 3b and d), also close to their charge ratio. Taking these results together, the electrostatic nanoassembly of **Pt-bzimpy-T** was formed at a **T/Pt-bzimpy** molar ratio of 1:3. At this ratio, the <sup>3</sup>MMLCT emission intensity was multiplied by a factor of 14 (Fig. S1). Such significant increase in the intensities of both

MMLCT absorption and <sup>3</sup>MMLCT emission bands were consequently attributed to the formation of aggregates of **Pt-bzimpy**.<sup>9,10</sup> In the DLS plot of **Pt-bzimpy-T**, two modes were observed with  $D_h$ s of 480 and 9100 nm (Fig. 2a). Both TEM and fluorescence microscope images showed that **Pt-bzimpy-T** formed sheet-like aggregates (Fig. 2c and d). As observed from the folded part, the thickness of the sheet was estimated to be ~20 nm (Fig. S2a and b). These aggregates should originate from a cooperative combination of electrostatic attractions, hydrogen bonds and intermolecular associations through Pt...Pt and  $\pi$ - $\pi$  stacking interactions. In sharp contrast, the mixture of **Pt-bzimpy** with **S** did not show significant <sup>3</sup>MMLCT luminescence enhancement due to the weaker hydrogen bonds and electrostatic attractions (Fig. S1).

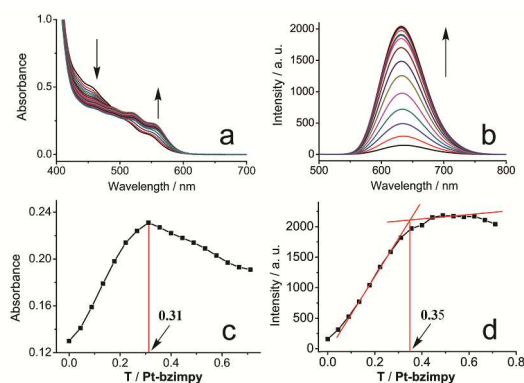


**Fig. 3** (a) Absorption and (b) emission spectra of **Pt-bzimpy** (0.15 mM) upon titration with **T**. Plots of (c) absorbance at 553 nm and (d) emission at 632 nm against the concentration ratio of **T** and **Pt-bzimpy**.

The temperature-dependent emission spectra of **Pt-bzimpy-T** were recorded from 25 to 95 °C. The <sup>3</sup>MMLCT luminescence band disappeared completely after heating to 80 °C (Fig. S3a). After the solution was cooled back to 25 °C, the emission intensity recovered only 70 %. This signal loss was attributed to the partial pyrohydrolysis of the reversible acylhydrazone bonds. The solution of **Pt-bzimpy-T** were further titrated with hydrochloric acid at pH values of 0.8~7. The titration results indicated that the acylhydrazone bonds were stable at pH 4~7 (Fig. S3b). 2-Formylbenzenesulfonic acid has a small pKa (-0.97±0.18).<sup>11</sup> Thus, most **T** molecules were expected to keep anionic forms in the present pH range. Interestingly, as a result of acylhydrazone hydrolysis, the luminescence intensity of **Pt-bzimpy-T** reached a minimum value of 1420 in 20 min at pH 2, relative to the initial emission intensity of 2080 (Fig. S3c). We therefore estimated a hydrolytic yield of 32 %. However, under the same condition, the hydrolytic equilibrium of pure **T** in D<sub>2</sub>O required only 10 min as shown in the integral curve of -CH=N- monitored by <sup>1</sup>H NMR spectra (Fig. S3d). The resulting hydrolytic yield was accordingly calculated to be 36 %, which agreed well with that obtained from the above-mentioned luminescence measurement. The slower hydrolysis of **T** in the presence of **Pt-bzimpy** should be ascribed to two possibilities: (1) The **Pt-bzimpy** cations could serve as a steric barrier to hinder the

hydrolytic reaction of **T** with  $H^+$ ; (2) The enhanced hydrophobicity of the electrostatic complex could repulse the attack of  $H^+$ .

To control luminescence behaviors of **Pt-bzimpy** via component exchanges of dynamic acylhydrazone bonds, **A1** and **H1** (9 equiv per **T**) were respectively added to the solutions of **Pt-bzimpy-T** (**Pt-bzimpy**, 0.45 mM and **T**, 0.15 mM) at pH 4. The  $^3\text{MMLCT}$  emission intensities showed a gradual decrease in both cases (Fig. 4a and b). After 68 hours, they respectively reached their minimum values of 46% and 22% of the initial luminescence (Fig. S4a and b). However, the  $^3\text{MMLCT}$  emission band is stable under this acid condition in the absence of exchange reagents (Fig. S3b). Similar exchanges were also tested at pH 2. At identical concentrations, aldehyde exchange reached an equilibrium after 100 min and luminescence intensity was reduced to 23 % of its initiative. As for hydrazine exchange, the equilibrium time was shortened to 40 min and the residual emission intensity was estimated to be 23 % (Fig. S5a and b). Evidently, the stronger acidity accelerated the acylhydrazone exchange reactions.<sup>1a</sup>

When the aldehyde exchange reached the equilibrium at pH 4, the DLS plot revealed two modes with  $D_n$ s at 1 and 280 nm, demonstrating the disruption of the aggregates of **Pt-bzimpy-T** (Fig. 5b). Taking account of the 46 % luminescence remainder, the latter DLS signal could be due to an incomplete exchange. TEM imaging still captured the membranous nanostructures (Fig. S6a). In comparison, hydrazine exchange completely destroyed the sheet-like nanoassembly as shown in the DLS plot (Fig. S7b) and TEM image (Fig. S8a), which was in accordance with the emission remainder of 22 %.

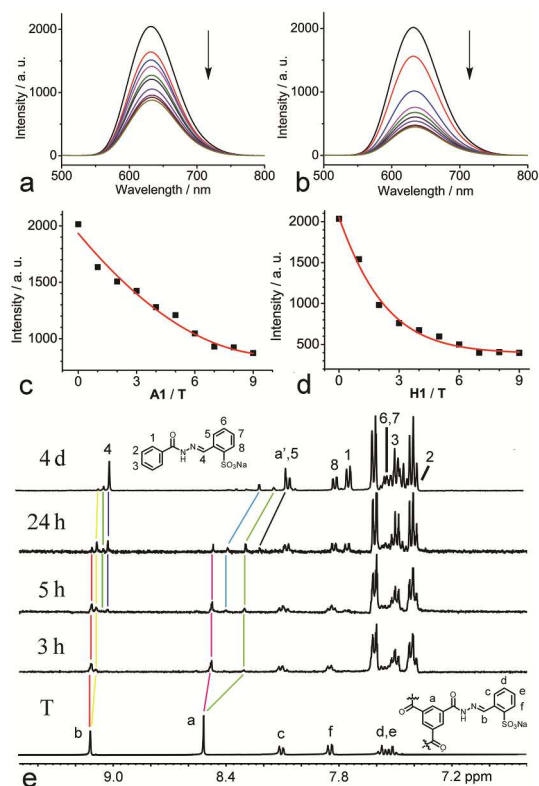


**Fig. 4** Emission spectra of **Pt-bzimpy-T** (**Pt-bzimpy**, 0.45 mM and **T**, 0.15 mM) upon titration with (a) **A1** and (b) **H1** at pH 4. The plots of luminescence intensities at 632 nm versus the molar ratios of (c) **A1/T** and (d) **H1/T**. (e)  $^1\text{H}$  NMR spectra of component exchanges upon addition of 9 equiv **H1** to a  $\text{D}_2\text{O}$  solution of **T** (4 mM) at pH 4. From bottom to top: pure **T**, **T** + **H1** at 3 h, 5 h, 24 h and 4 d.

$^1\text{H}$  NMR spectra were carried out to analyze the process of component exchanges. In order to avoid the resonance interferences of **Pt-bzimpy** in the low field region, pure **T** was selected for the simplified study. As shown in Fig. 4e, time-dependent  $^1\text{H}$  NMR spectra were recorded upon addition of **H1** (9 eq) to a  $\text{D}_2\text{O}$  solution of **T** (4 mM) at pH 4. The resonance signals of the aromatic proton  $H_a$  (8.54 ppm) and imine proton  $H_b$  (9.14 ppm) in **T** disappeared gradually, indicating that the hydrolysis of the tripodal acylhydrazone bonds proceeded. At the reaction stages of 3 and 5 h, the resonances of  $H_a$  and  $H_b$  were splitted into the signals at (8.30 and 8.41 ppm) and (9.09 and 9.05 ppm), respectively. These splitted signals revealed that one and two acylhydrazone bonds were hydrolyzed successively. After 24 h, the resonance signal at 8.22 ppm was attributed to the aromatic proton of 1,3,5-tricarbohydrazone benzene, indicative of the formation of the final hydrolysate. The resonance signal of  $H_4$  (9.03 ppm) clearly revealed the generation of **S** at 5 h. Furthermore, the high-resolution electrospray ionization mass spectrum (HR-ESI-MS) confirmed the presence of **S** at an  $m/z$  of 303.0460 (calcd 303.0445). The  $^1\text{H}$  NMR peaks of **S** were gradually intensified at the expense of **T** and its hydrolytic products. Finally, characteristic signals of both **S** and excess **H1** predominated in the  $^1\text{H}$  NMR spectrum after 4 days. These  $^1\text{H}$  NMR data evidenced the hydrazine exchange and were essentially consistent with the results of the luminescence, DLS, and TEM measurements. Upon the addition of aldehyde **A1** instead of **H1**, similar exchange equilibrium was formed within 4 days at pH 4 (Fig. S9). Consistent with the luminescence data, the  $^1\text{H}$  NMR spectra also described an incomplete exchange.

These results indicated: (1) The replacement of 2-formylbenzenesulfonate by **A1** lowered the negative charge number in the nanoassembly of **T** and thus the corresponding electrostatic attractions between **T** and **Pt-bzimpy**; (2) After addition of **H1**, the exchange product **S** had only one hydrazine bond and thus was insufficient to construct the aggregates of **Pt-bzimpy** (Fig. S10a and b). The plots of the emission intensities ( $y$ ) at 632 nm versus the molar ratios ( $x$ ) of **A1/T** or **H1/T** showed a nonlinear relationship (Fig. 4c and d), where  $a$ ,  $b$ ,  $c$ , and  $d$  were constants. They were respectively

$$y = a + \frac{b}{1 + e^{(cx+d)}}$$

determined to be 626,  $6.36 \times 10^5$ , 0.185, and 6.16 for the aldehyde exchange. In the hydrazine-exchange reactions, they were determined to be 456, 7309, 0.535, and 1.214 (Table S1). This equation allowed us to estimate the luminescence outputs of the exchange reaction systems. Conversely, desired emission intensity can be achieved via the quantitative addition of exchange reagents.

After having investigated these primary exchanges of the acylhydrazone bond, we in situ added **A2** (9 equiv per **A1**) to the aldehyde exchange system mentioned above. A new thermodynamic equilibrium evolved at pH 4 after 4 days. The  $^1\text{H}$  NMR spectra indicated that the acylhydrazone derivative decorated with hexaethylene glycol methyl ether groups was retransformed into **T** (Fig. 5a). The corresponding emission intensity recovered to 78 % in comparison with the initial one (Fig. 5b), which was presumably ascribed to the generation of by-products and incomplete exchanges. Meanwhile,  $D_n$  increased to 350 nm (Fig. 5c). No regular aggregates were observed in the TEM image (Fig. S6b), which could be due to abundant **A1** and **A2** in the solutions. In comparison, **T** wasn't regenerated upon the addition of **H2** (9 equiv per **H1**) to the hydrazine exchange system as confirmed by  $^1\text{H}$  NMR spectra (Fig. S7a). Some new resonance signals presumably arose from a mixture of possible amins and hemiaminals.<sup>12</sup> Furthermore, the luminescence was quenched completely (Fig. S7b). Accordingly, large size particles were not observed in both the DLS plot (Fig. S7c) and TEM image (Fig. S8b).

In conclusion, the electrostatic self-assembly of a tripodal dynamic acylhydrazone-bridged sulfonate with a cationic chloroplatinum(II) complex leads to the formation of aggregates and thus remarkable  $^3\text{MMLCT}$  luminescence enhancement in aqueous solution. By virtue of hydrolysis and component exchange of the acylhydrazone bonds under acidic conditions, the  $^3\text{MMLCT}$  emission was programmably controlled. The introduction of dynamic covalent bonds into metallosupramolecular systems represents a new approach to develop luminescence soft materials with tunable optical outputs.

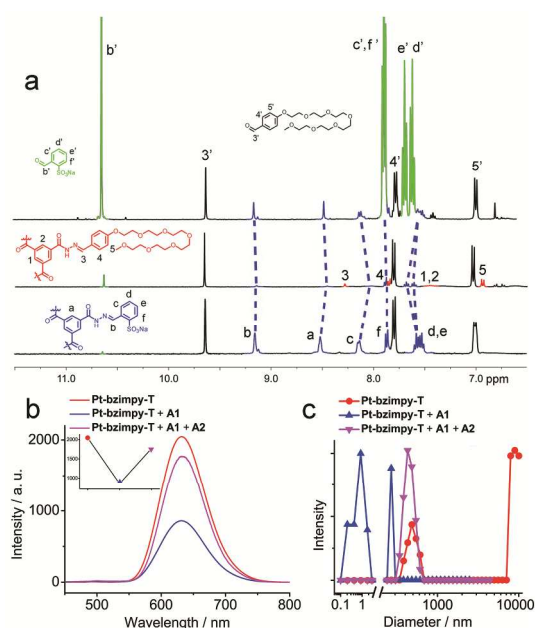


Fig. 5 (a)  $^1\text{H}$  NMR profiles of twice aldehyde exchanges upon additions of 9 equiv **A1** and 81 equiv **A2** to **T** (4 mM) at pH 4. (b) Luminescence and (c) DLS plots of twice aldehyde exchanges upon additions of 9 equiv **A1** and 81 equiv **A2** per **T** to **Pt-bzimpy-T** (**Pt-bzimpy-T**, 0.45 mM and **T**, 0.15 mM) at pH 4.

This work is supported by the NSFC (51173073 and J1103307), the Fundamental Research Funds for the Central Universities (Izujbky-2013-238 and Izujbky-2014-74) and the Open Project of State Key Laboratory of Supramolecular Structure and Materials of Jilin University (sklssm201405).

### Notes and references

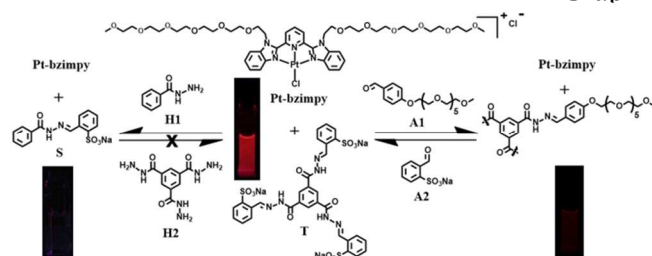
Key Laboratory of Nonferrous Metals Chemistry and Resources Utilization of Gansu Province, State Key Laboratory of Applied Organic Chemistry, College of Chemistry and Chemical Engineering, Lanzhou University, Lanzhou City, Gansu Province, China. Fax: +86 931 8912582, E-mail: [buwf@lzu.edu.cn](mailto:buwf@lzu.edu.cn)

† Electronic Supplementary Information (ESI) available: Synthesis and analysis details of **T**, **S** and **A1** and additional characterizations. See DOI: 10.1039/b000000x/

- (a) P. T. Corbett, J. Leclaire, L. Vial, K. R. West, J.-L. Wietor, J. K. M. Sanders, S. Otto, *Chem. Rev.*, 2006, **106**, 3652; (b) J.-M. Lehn, *Chem. Soc. Rev.*, 2007, **36**, 151; (c) Y. Jin, C. Yu, R. J. Denman, W. Zhang, *Chem. Soc. Rev.*, 2013, **42**, 6634; (d) A. Wilson, G. Gasparini, S. Matile, *Chem. Soc. Rev.*, 2014, **43**, 1948.
- (a) S. J. Rowan, S. J. Cantrill, G. R. L. Cousins, J. K. M. Sanders and J. F. Stoddart, *Angew. Chem. Int. Ed.*, 2002, **41**, 898; (b) M. E. Belowich and J. F. Stoddart, *Chem. Soc. Rev.*, 2012, **41**, 2003; (c) J. Boekhoven, J. M. Poolman, C. Maity, F. Li, L. van der Mee, C. B. Minkenberg, E. Mendes, J. H. van Esch and R. Eelkema, *Nat. Chem.*, 2013, **5**, 433.
- (a) V. T. Bhat, A. M. Caniard, T. Luksch, R. Brenk, D. J. Campopiano and M. F. Greaney, *Nat. Chem.*, 2010, **2**, 490; (b) M. Mondal, N. Radeva, H. Köster, A. Park, C. Potamitis, M. Zervou, G. Klebe and A. K. H. Hirsch, *Angew. Chem. Int. Ed.*, 2014, **53**, 3259; (c) A. Herrmann, *Angew. Chem. Int. Ed.*, 2007, **46**, 5836.
- (a) M. von Delius, E. M. Geertsema, D. A. Leigh, *Nat. Chem.*, 2010, **2**, 96; (b) M. S. Congreve, D. J. Davis, L. Devine, C. Granata, M. O'Reilly, P. G. Wyatt and H. Jhoti, *Angew. Chem. Int. Ed.*, 2003, **42**, 4479; (c) B. de Bruin, P. Hauwert and J. N. H. Reek, *Angew. Chem. Int. Ed.*, 2006, **45**, 2660.
- (a) S. Choudhary and J. R. Morrow, *Angew. Chem. Int. Ed.*, 2002, **41**, 4096; (b) M.-K. Chung, P. S. White, S. J. Lee and M. R. Gagne, *Angew. Chem. Int. Ed.*, 2009, **48**, 8683; (c) L. Mugerli, O. N. Burchak, L. A. Balakireva, A. Thomas, F. Chatelain and M. Y. Balakirev, *Angew. Chem. Int. Ed.*, 2009, **48**, 7639; (d) G. Gasparini, L. J. Prins and P. Scrimin, *Angew. Chem. Int. Ed.*, 2008, **47**, 2475.
- (a) I. Eryazici, C. N. Moorefield, G. R. Newkome, *Chem. Rev.*, 2008, **108**, 1834; (b) S. D. Cummings, *Coord. Chem. Rev.*, 2009, **253**, 449; (c) R. McGuire Jr, M. C. McGuire, D. R. McMillin, *Coord. Chem. Rev.*, 2010, **254**, 2574; (d) J. Kalinowski, V. Fattori, M. Cocchi, J. A. G. Williams, *Coord. Chem. Rev.*, 2011, **255**, 2401; (e) X. Zhang, B. Li, Z.-H. Chen, Z.-N. Chen, *J. Mater. Chem.*, 2012, **22**, 11427; (f) K. M. C. Wong, V. W.-W. Yam, *Acc. Chem. Res.*, 2011, **44**, 424; (g) T. J. Wadas, Q.-M. Wang, Y.-j. Kim, C. Flaschenreim, T. N. Blanton, R. Eisenberg, *J. Am. Chem. Soc.*, 2004, **126**, 16841; (h) L. J. Grove, J. M. Rennekamp, H. Jude, W. B. Connick, *J. Am. Chem. Soc.*, 2004, **126**, 1594; (i) E. J. Rivera, C. Figueroa, J. L. Colón, L. Grove, W. B. Connick, *Inorg. Chem.*, 2007, **46**, 8569; (j) A. Y.-Y. Tam, D. P.-K. Tsang, M.-Y. Chan, N. Zhu and V. W.-W. Yam, *Chem. Commun.*, 2011, **47**, 3383.

- 7 (a) D. R. McMillin, J. J. Moore, *Coord. Chem. Rev.*, 2002, **229**, 113; (b) S. E. Hobert, J. T. Carney, S. D. Cummings, *Inorg. Chim. Acta*, 2001, **318**, 89; (c) M. C.-L. Yeung, V. W.-W. Yam, *Chem.–Eur. J.*, 2011, **17**, 11987; (d) C. Yu, K. H. Y. Chan, K. M. C. Wong, V. W.-W. Yam, *Proc. Natl. Acad. Sci. U. S. A.*, 2006, **103**, 19652; (e) C. Yu, K. M. C. Wong, K. H. Y. Chan, V. W.-W. Yam, *Angew. Chem., Int. Ed.*, 2005, **44**, 791; (f) C. Yu, K. H. Y. Chan, K. M.-C. Wong, V. W.-W. Yam, *Chem.–Eur. J.*, 2008, **14**, 4577; (g) K. H.-Y. Chan, J. W.-Y. Lam, K. M.-C. Wong, B.-Z. Tang, V. W.-W. Yam, *Chem.–Eur. J.*, 2009, **15**, 2328; (h) K.-Y. Wong, W. W.-S. Lee, *J. Photochem. Photobiol. A*, 1997, **102**, 231; (i) N. A. Larew, A. R. V. Wassen, K. E. Wetzel, M. M. Machala, S. D. Cummings, *Inorg. Chim. Acta*, 2010, **363**, 57.
- 8 (a) C. Y. S. Chung, V. W.-W. Yam, *J. Am. Chem. Soc.*, 2011, **133**,

## Graphical Abstract



### Tuning luminescence behaviors of a chloroplatinum(II) complex by component exchanges of dynamic acylhydrazone bond

Jianjun Liang, Huanting Huang, Lipeng He, Nijuan Liu, Yanhuan Chen and Weifeng Bu\*

The exchange reactions of dynamic acylhydrazone bonds with acylhydrazine or aldehyde lead to controllable emissions of a cationic chloroplatinum(II) complex in water.

- 18775; (b) N. Liu, B. Wang, W. Liu, W. Bu, *Chem. Commun.*, 2011, **47**, 9336; (c) N. Liu, B. Wang, W. Liu, W. Bu, *J. Mater. Chem. C*, 2013, **1**, 1130.
- 9 J. Liang, X. Zheng, L. He, H. Huang, W. Bu, *Dalton Trans.*, 2014, **43**, 13174.
- 10 J. J. van Gorp, J. A. J. M. Vekemans, E. W. Meijer, *J. Am. Chem. Soc.*, 2002, **124**, 14759.
- 11 Calculated using Advanced Chemistry Development (ACD/Labs) Software V11.02 (© 1994-2014 ACD/Labs).
- 12 Nguyen, R. Ivan Huc, *Chem. Commun.*, 2003, **39**, 942.